Cellular and Molecular Life Sciences

RESEARCH ARTICLE

Cilioplasm is a cellular compartment for calcium signaling in response to mechanical and chemical stimuli

Xingjian Jin · Ashraf M. Mohieldin ·
Brian S. Muntean · Jill A. Green · Jagesh V. Shah ·
Kirk Mykytyn · Surya M. Nauli

Abstract Primary cilia with a diameter of ~200 nm have been implicated in development and disease. Calcium signaling within a primary cilium has never been directly visualized and has therefore remained a speculation. Fluid-shear stress and dopamine receptor type-5 (DR5) agonist are among the few stimuli that require cilia for intracellular calcium signal transduction. However, it is not known if these stimuli initiate calcium signaling within the cilium or if the calcium signal originates in the cytoplasm. Using an integrated single-cell imaging technique, we demonstrate for the first time that calcium signaling triggered by fluid-shear stress initiates in the primary cilium and can be distinguished from the subsequent cytosolic calcium response through the ryanodine receptor. Importantly, this flow-induced calcium signaling depends on the ciliary polycystin-2 calcium channel. While DR5-specific agonist induces calcium signaling mainly in the cilioplasm via ciliary CaV1.2, thrombin specifically induces cytosolic calcium signaling through the IP_3 receptor. Furthermore, a non-specific calcium ionophore triggers both ciliary and cytosolic calcium responses. We suggest that cilia not only act as sensory organelles but also function as calcium signaling compartments. Cilium-dependent signaling can spread to the cytoplasm or be contained within the cilioplasm. Our study thus provides the first model to understand signaling within the cilioplasm of a living cell.

Keywords Chemosensing · Ciliopathy · Mechanosensing · Microscope · Microwire · Polycystic kidney

X. Jin · S. M. Nauli
Department of Medicine, College of Medicine, The University of Toledo, Toledo, OH 43606, USA

A. M. Mohieldin · B. S. Muntean · S. M. Nauli
Department of Pharmacology, College of Pharmacy and Pharmaceutical Sciences, The University of Toledo, Toledo, OH 43606, USA

J. A. Green · K. Mykytyn
Department of Pharmacology, College of Medicine, The Ohio State University, Columbus, OH 43210, USA

J. V. Shah
Department of Systems Biology, Harvard Medical School and Renal Division, Brigham and Women's Hospital, Boston, MA 02115, USA

S. M. Nauli (✉)
Department of Pharmacology, MS 1015, Health Education Building, Room 282D, The University of Toledo, 3000 Arlington Ave, Toledo, OH 43614, USA
e-mail: surya.nauli@utoledo.edu

Introduction

Primary cilia are microtubule-based organelles found on the apical surface of most mammalian cell types. The sensory functions of primary cilia in the kidney are generally characterized into mechano- [1–9] and chemosensation [10–13]. The hypothesis of mechanosensory cilia is based on the observation that cilia bend when subjected to fluid flow [14], resulting in changes in cytosolic calcium levels [6]. Moreover, many laboratories have shown that fluid-shear stress and a few pharmacological agents depend on primary cilia for intracellular signaling, including calcium signaling [1–13]. Due to the size of primary cilia with a diameter of ~200 nm, however, there has never been a

direct visualization of any signaling occurring within the primary cilium. Worth mentioning is that most primary cilia are oriented perpendicular to the cell surface, which makes visualizing ciliary signaling in live cells extremely challenging, in addition to the tiny diameter of primary cilia.

Because abnormal primary cilia have been associated with a long list of clinical pathologies [15], it is extremely crucial to examine signaling pathways in the cilia of distinct living cells. Measuring a specific signal explicitly within a cilium would allow a precise interpretation of the ciliary functions. In addition, it would provide important insight into the dynamics of signaling between the cilium and cell body. In other words, many cilium-dependent responses have only been detected at the cellular level or in fixed tissues, resulting in uncertainty of how ciliary signal transduction propagates from the cilium as a sensory organelle to the cell body as a whole.

In the present study, we adopted a new integrated single-cell imaging technique to distinctively visualize the cilium (cilioplasm) and the cell body (cytoplasm). For the first time, we provide differential visual evidence of the cilium-dependent and cilium-independent signaling mechanisms in a living cell. Our data demonstrate that fluid-shear stress and dopamine receptor-type 5 (DR5) agonist generate calcium fluxes in the cilioplasm through distinct ciliary calcium channels polycystin-2 and CaV1.2, respectively. While thrombin induces calcium signaling mainly in the cytoplasm, ionomycin generates non-specific calcium increases in cilioplasm and cytoplasm.

Results

### Precision microwire allows differential visualization of CTS-G-CaMP3 in the cilioplasm and cytoplasm

None of the calcium-sensitive fluorophores are loaded into the cilioplasm (data not shown). To visualize calcium signaling within the cilium, we therefore fused G-CaMP3 with a highly conserved cilia-targeting sequence (CTS) that was identified in the fibrocystin protein [16]. To test the specificity of our CTS-G-CaMP3 construct, we also examined the localization of G-CaMP3 lacking the CTS. Whereas G-CaMP3 shows only cytosolic localization, CTS-G-CaMP3 localizes to both the cytosol and cilia of fixed LLCPK cells, as indicated colocalization with the ciliary marker acetylated-α-tubulin (Fig. 1).

To allow us to observe cultured cells from the side, we adopted a differential side-view imaging platform using

Fig. 1 CTS-G-CaMP3 is co-localized with acetylated-α-tubulin in primary cilia LLCPK cells were fixed, permeabilized and immuno-stained with the ciliary marker acetylated-α-tubulin (acet-α-tub). Non-transfected cells show no green fluorescence signal and are used as a negative control (*upper row*). Cells transfected with G-CaMP3 show green fluorescence signal only in the cell body (*middle row*). CTS-G-CaMP3 transfected cells show green fluorescence signal in the cilium (*lower row*), as indicated by the ciliary marker (*red fluorescent*). Merged images of *green* and *red* signals are shown with DAPI (nuclear DNA staining). *Bar* = 4 μm
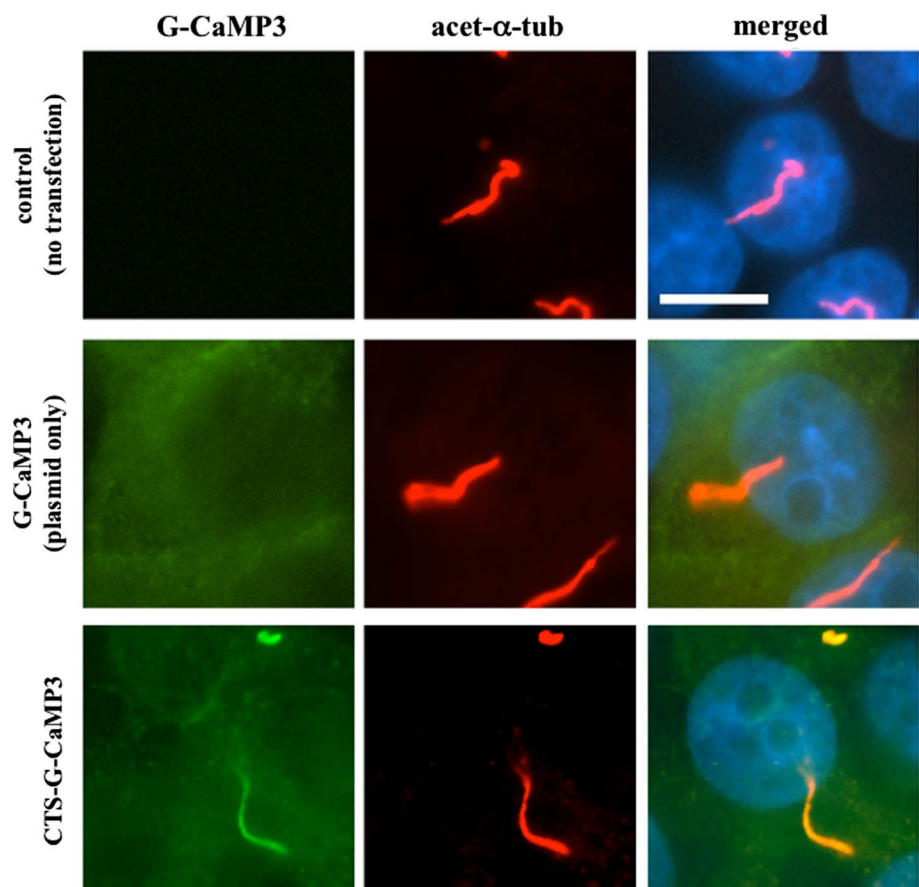
Fig. 2 CTS-G-CaMP3 is localized to the cilium in live cells. A live LLCPK cell was imaged from the side using high-resolution differential interference contrast (DIC) and fluorescence microscopy. **a** A Tungsten precision microwire with a diameter of 100 μm was coated with collagen (*upper row*). Cells were seeded and selectively grew around the wire (*lower row*). **b** A non-transfected cell displays no fluorescence signal (control; *upper row*). Background autofluorescent from the microwire can be occasionally seen. A cell transfected with G-CaMP3 shows fluorescence only in the cell body (*middle row*). A CTS-G-CaMP3 transfected cell shows fluorescence signal in the cell body and cilium (*lower row*). *Black bar* = 50 μm, *white bar* = 4 μm
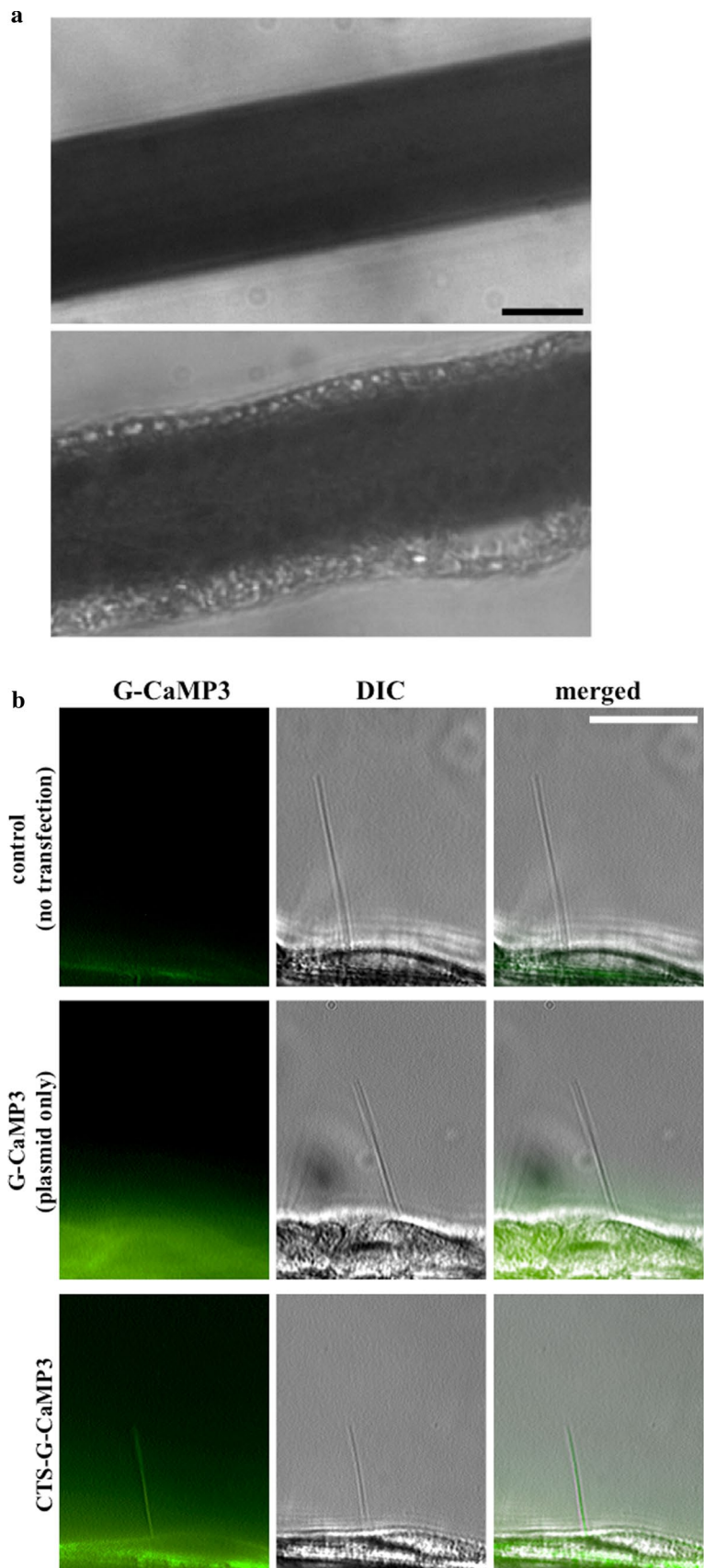
precision microwire to overcome the issues with optical distortions of traditional two-dimensional live-cell imaging. Renal epithelial cells were grown on a specially made Tungsten wire with a purity of greater than 99.9 % and a standardized diameter of 100 μm. Using precision microwire, we are able to perform a differential side-view imaging of individual cells (Fig. 2a). To determine if our CTS-G-CaMP3 construct is expressed and localizes to cilia in cells grown on the intended platform, we re-examined the G-CaMP3 fluorescence signal in live LLCPK cells (Fig. 2b). Live-cell imaging demonstrates that the non-transfected cells have no specific fluorescence signal. As expected, G-CaMP3-transfected cells show a fluorescence signal only in the cytoplasm, but the CTS-G-CaMP3 signal can be observed in the cilioplasm and cytoplasm. The localization of CTS-G-CaMP3 in cilia and cytosol may be a consequence of high expression levels of CTS-G-CaMP3; it may also be due to the fact that fibrocystin is expressed in both cilia and cytosol [17]. Nevertheless, the nature of this subcellular localization allows us to measure both ciliary and cytosolic calcium levels differentially and simultaneously.

Flow-induced ciliary calcium depends on polycystin-2 and propagates to the cytoplasm via the ryanodine receptor

To determine whether bending of cilia results in increased ciliary calcium, we applied fluid-shear stress of 0.7 dyne/cm², which has been previously shown to activate cilium-dependent intracellular calcium signaling [3, 5]. This magnitude of shear stress also allows optimal physical bending of a cilium (Fig. 3a; Movie 1). In the presence of fluid-shear, the bending of the cilium induces an increase in ciliary calcium levels (Movies 2 and 3). The increase in ciliary calcium is then followed by an increase in cytosolic calcium. While inhibiting IP3 receptor with 2-APB (10 μM) does not have any major effect on flow-induced ciliary or cytosolic calcium increase (Fig. 3b), blocking the ryanodine receptor with caffeine (60 μM) distinctively abolishes cytosolic calcium, while ciliary calcium is still increased by fluid-flow (Fig. 3c). Our study also shows that polycystin-2 is involved in flow-induced intracellular calcium increases in both cilioplasm and cytoplasm (Fig. 3d). As indicated by our Cy5-tagged *Pkd2* siRNA, we have a transfection frequency of about 80 %. This Cy5-tagged strategy also allows us to selectively pick a successfully transfected cell for live imaging. Overall quantitation indicates that polycystin-2 and ryanodine receptor are differentially and distinctively involved in subcellular calcium signaling in response to fluid-shear stress (Fig. 3e).

We next examined the effect of *Pkd2* siRNA on polycystin-2 expression (Fig. 3f). Either 20 or 30 nM of *Pkd2*

Fig. 3 Flow-induced calcium signaling originates from the cilium. ▶ DIC and fluorescence images were captured simultaneously. Representative DIC images are to show the bending of cilia by fluid-shear stress. Representative calcium signaling in the cilioplasm and cytoplasm was then differentially observed for each group. Quantitation analysis from 3–6 independent experiments was averaged and plotted in the line graphs for cilioplasm and cytoplasm. **a** Fluid-shear induces calcium signaling in the cilioplasm followed by signaling in the cytoplasm. Representative fluorescent images from two separate flow experiments are shown. **b** Pre-incubation with 2-APB for 30 min has a minimal effect on ciliary or cytosolic calcium. **c** Pre-incubation with caffeine for 30 min specifically inhibits the cytosolic calcium increase in response to fluid-shear. **d** A cell transfected with *Pkd2* siRNA tagged with Cy5 shows no ciliary or cytosolic calcium changes in response to fluid-shear. A transfected cell is indicated by the presence Cy5 fluorescence (*red*). **e** Statistical analysis was done by analyzing the peak changes of intracellular calcium. *Asterisks* indicate differences compared to control scramble siRNA group. **f** Cells transfected with 20 or 30 nM *Pkd2* siRNA show a significant decrease in polycystin-2 (PC2) expression, compared to those with a scrambled siRNA. Time is indicated in seconds (s). *Color bar* indicates calcium level, where *black–purple* and *yellow–red* colors represent low and high calcium levels, respectively. *Bar* = 4 μm, n = 3–6 for each flow experiment and n = 4 for protein (siRNA) analysis

siRNA is sufficient to repress the overall expression of polycystin-2.

Differential subcellular calcium signaling provides a new paradigm of chemosensory role of renal epithelial cilia

Our group and others recently identified DR5 as a chemosensory receptor in cilia of endothelial and fibroblast cells [11, 18]. We therefore hypothesized that DR5-specific agonist, fenoldopam, can also trigger calcium signaling within the cilioplasm of renal epithelia. To test this hypothesis, we challenged the cells with 1 μM of fenoldopam (Fig. 4a; Movies 4 and 5). We found that fenoldopam specifically increases ciliary calcium levels with minimal calcium increase in the cytoplasm. To further understand the calcium channel involved in this response, we screened various inhibitors that would block DR5-induced ciliary calcium, including *Pkd2* siRNA. Surprisingly, 1 μM of verapamil sufficiently inhibits the effect of fenoldopam on ciliary calcium signal (Fig. 4b). Worth mentioning is that verapamil is generally known as a potent inhibitor of L-type calcium channel in the heart [19].
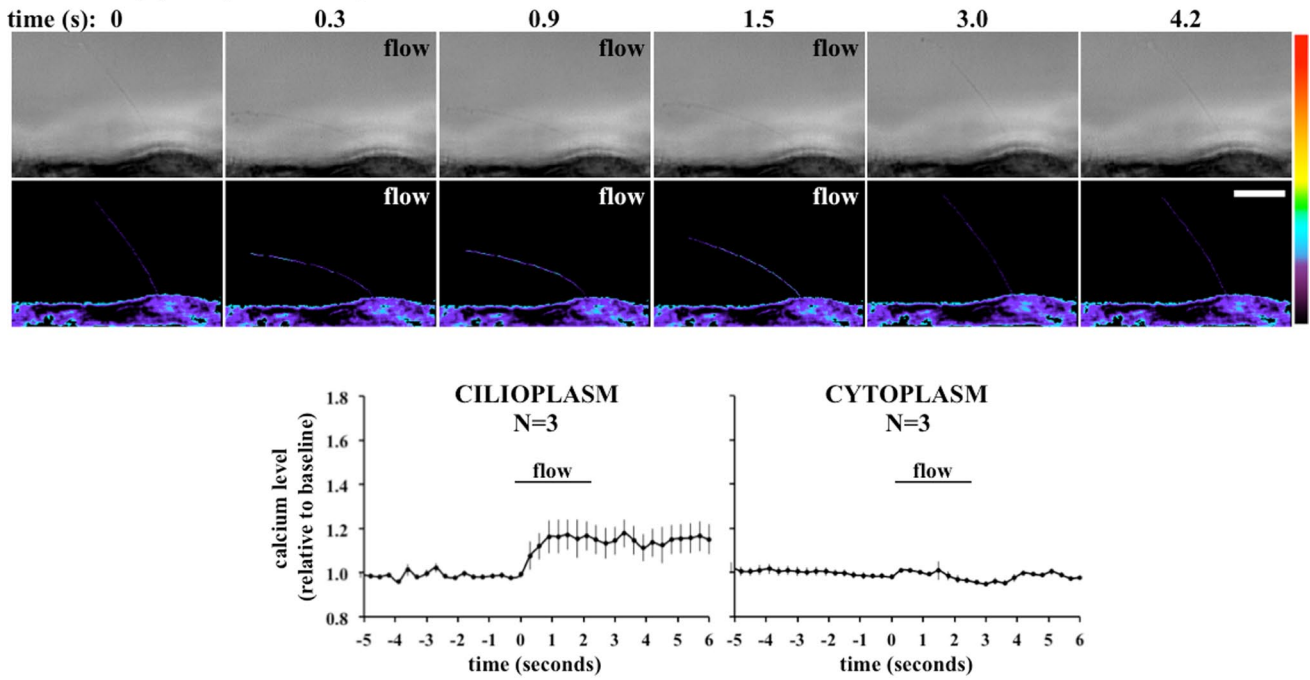
We previously confirmed that calcium signaling in response to thrombin or ionomycin is not a cilia-mediated signal transduction [3]. We thus challenged a cell with thrombin, a specific agonist for G-protein-coupled thrombin receptor, in the absence (Fig. 4c; Movies 6 and 7) or presence (Fig. 4d) of 10 μM 2-APB. While 1 μM of thrombin increases cytosolic calcium, the effect of thrombin is blocked by 2-APB, indicating the IP3 receptor is required for the thrombin-induced signal transduction pathway.

a control

time (s): 0   0.3   0.9   1.5   3.0   4.2
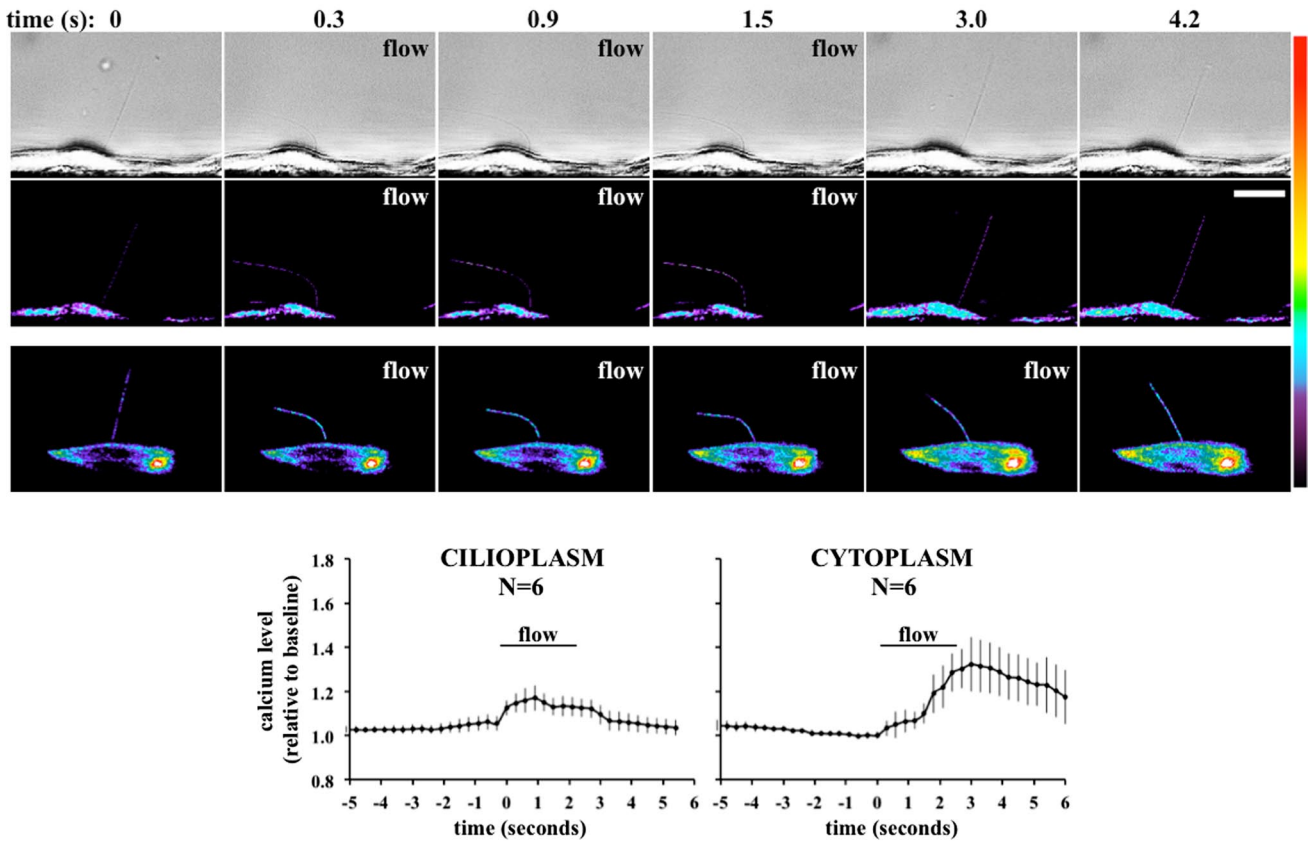
b 2APB (IP$_3$ receptor blocker)
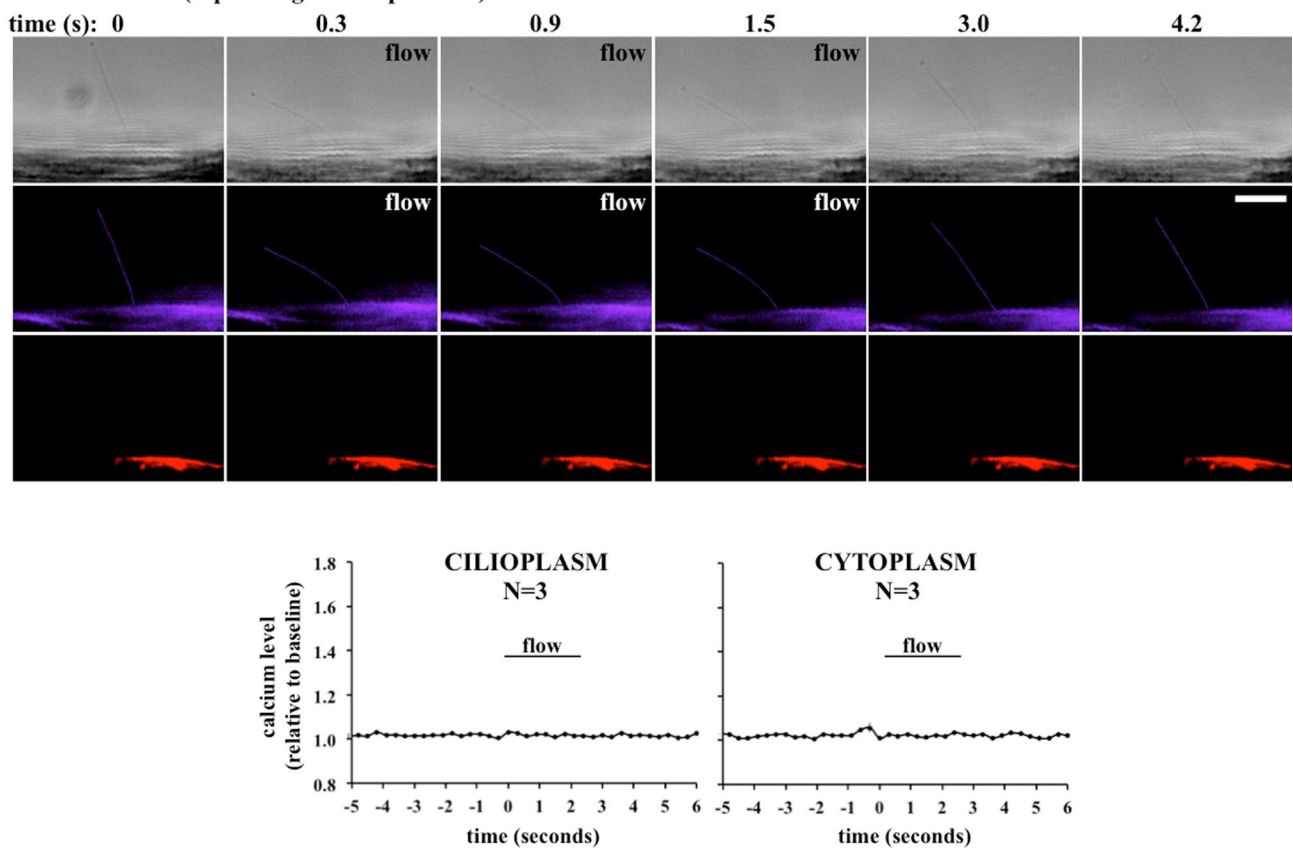
time (s): 0   0.3   0.9   1.5   3.0   4.2
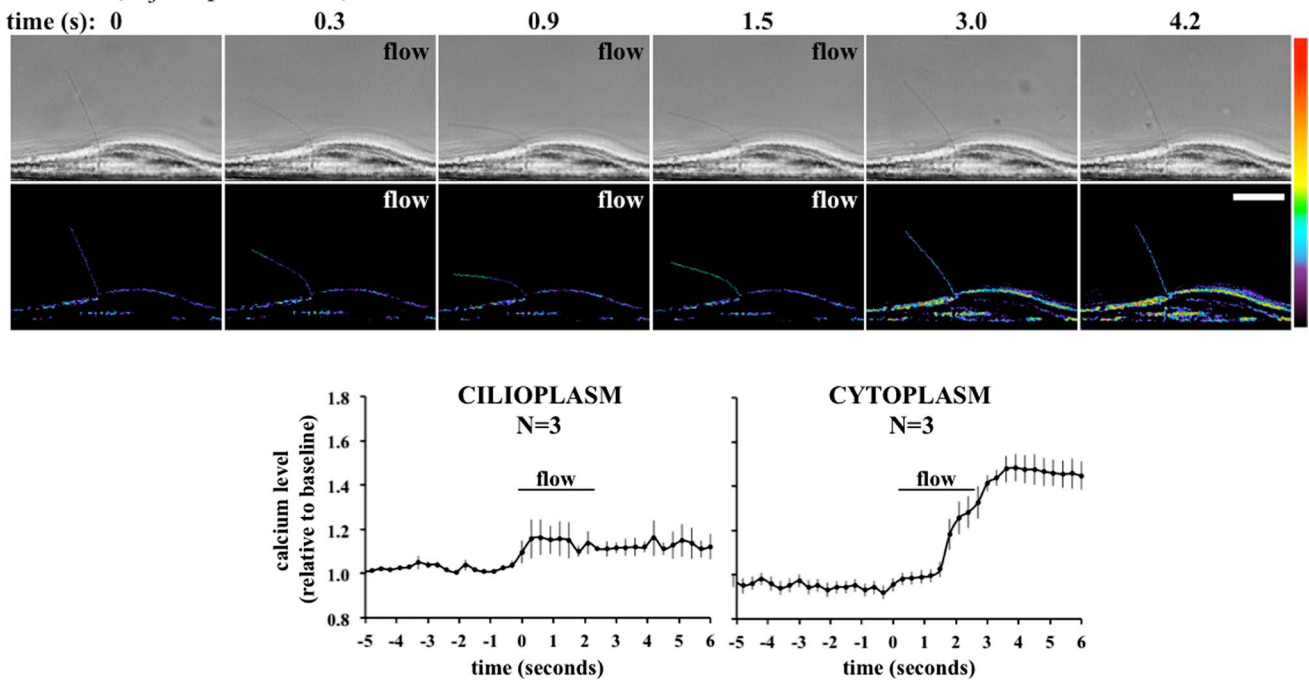
Unlike thrombin, which has no effect on ciliary calcium, 1 μM of ionomycin non-specifically increases calcium levels in both the cilioplasm and cytoplasm (Fig. 4e; Movies 8 and 9). Of note is that ionomycin as a non-selectivity calcium ionophore can function as our positive control in verifying our new experimental set-up.

c caffeine (Ry receptor blocker)

time (s):　0　　　　　0.3　　　　　0.9　　　　　1.5　　　　　3.0　　　　　4.2

d *Pkd2* siRNA (repressing PC2 expression)

time (s):　0　　　　　0.3　　　　　0.9　　　　　1.5　　　　　3.0　　　　　4.2

Fig. 3　continued

e **flow-induced calcium response (N=3-6)**

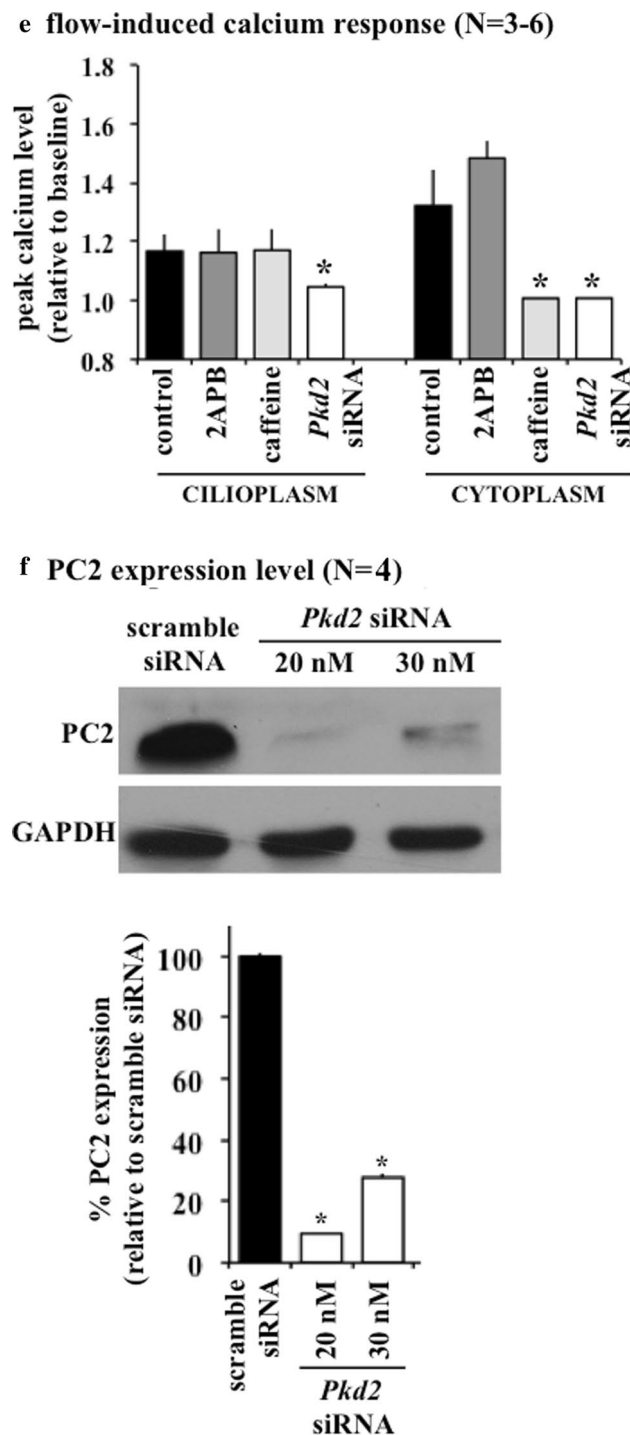**f** **PC2 expression level (N=4)**

Fig. 3 continued

Overall quantitation indicates that (1) fenoldopam increases ciliary calcium, and verapamil significantly represses this calcium change, (2) thrombin increases cytosolic calcium, and 2-APB significantly represses this increase, and (3) ionomycin increases a much greater cytosolic than ciliary calcium (Fig. 4f).

The L-type voltage-dependent calcium channel and dopamine receptor-type 5 are localized to primary cilia of renal epithelia

To elaborate more on the result of our chemical screening and the relationship between verapamil and fenoldopam
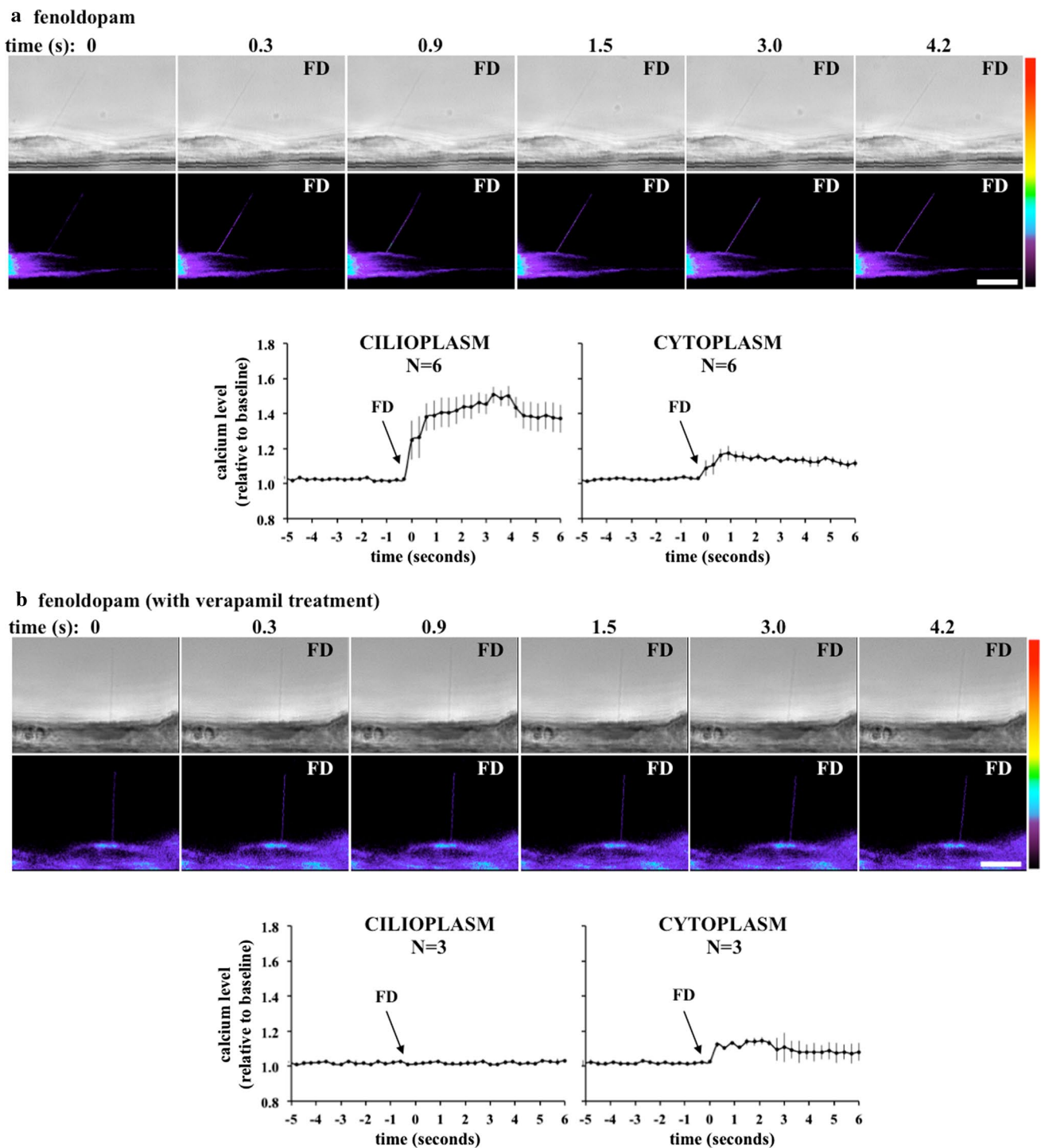
Fig. 4 Agonist-induced calcium signaling can occur in the cilioplasm and/or cytoplasm. Calcium signaling was analyzed using different agonists. Representative DIC and calcium images in each panel show that the primary cilium remained in focus throughout our studies, and calcium signaling in the cilioplasm and cytoplasm was differentially quantified for each group. Quantitation analysis from 3–6 independent experiments was averaged and plotted in the line graphs for cilioplasm and cytoplasm. **a** Fenoldopam (FD)-induced calcium signaling is more apparent in the cilioplasm than cytoplasm. **b** Pre-incubation with verapamil for 30 min ablates FD-induced ciliary calcium flux. **c** Thrombin (TH)-induced calcium signaling is specifically observed in the cytoplasm. **d** Pre-incubation with 2-APB for 30 min blocks TH-induced cytosolic calcium signaling. **e** The non-specific calcium ionophore, ionomycin (IO), induces calcium signaling simultaneously in the cilioplasm and cytoplasm. **f** Statistical analysis was done by analyzing the peak changes of intracellular calcium, where VA denotes verapamil. Time is indicated in seconds (s). *Color bar* indicates calcium level, where *black–purple* and *yellow–red* colors represent low and high calcium levels, respectively. *Bar* = 4 μm, *n* = 3–6 for each experiment

c thrombin

d thrombin (with 2APB treatment)
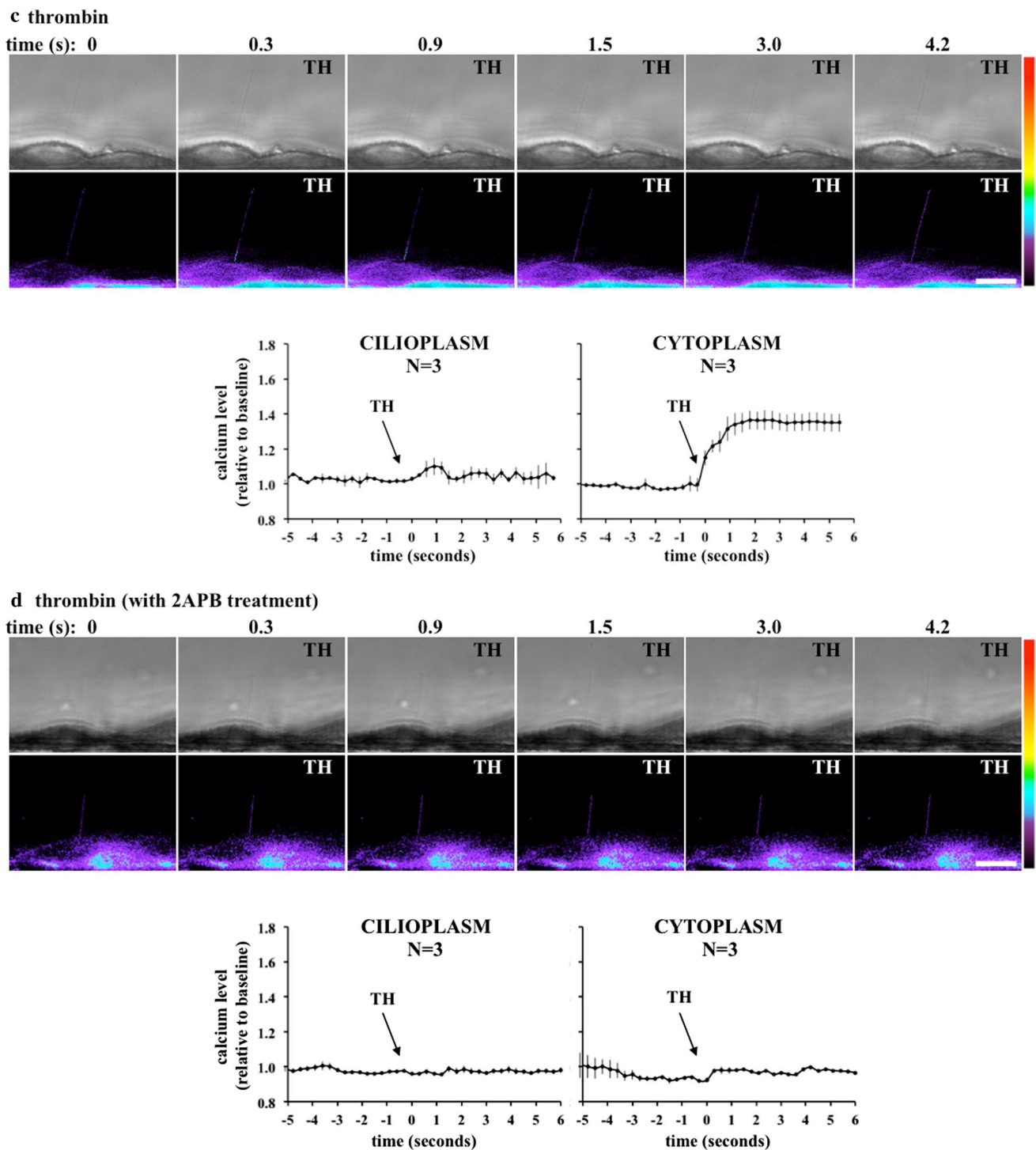
Fig. 4 continued

(Fig. 4b), we examined the possibility of the L-type calcium channel (CaV1.2) and dopamine receptor-type 5 (DR5) in the cilia. We here report for the first time that CaV1.2 is localized to renal epithelial cilia (Fig. 5a). Whereas DR5 is mainly localized to the primary cilia in renal epithelial (Fig. 5b), thrombin receptor is localized throughout the apical membrane (Fig. 5c). The immunolocalization data support the overall functional studies defining distinct subcellular calcium signaling within a single cell.
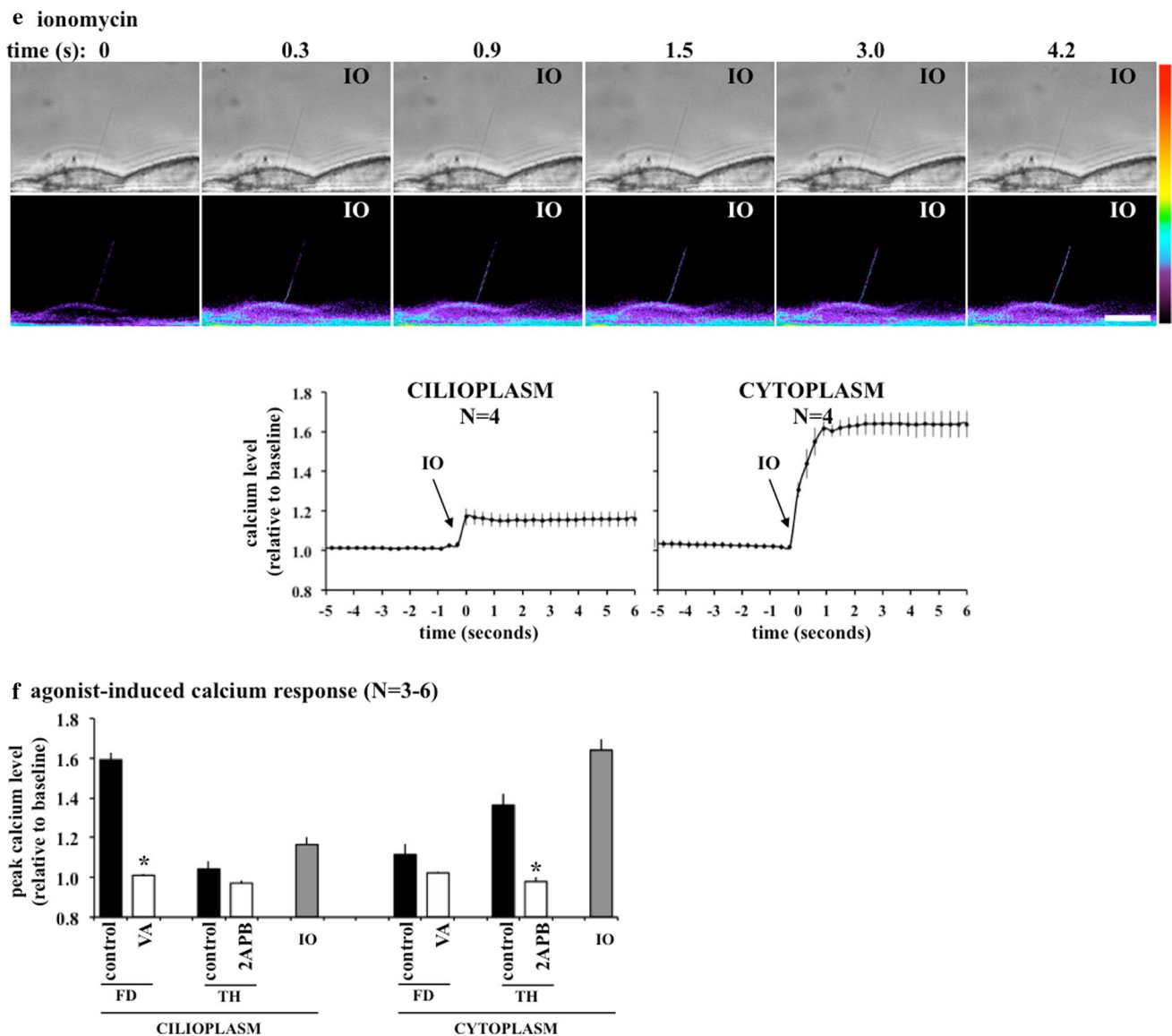
e ionomycin

f agonist-induced calcium response (N=3-6)

Fig. 4 continued

Discussion

Our present studies integrate three technologies to allow direct measurement of ciliary signaling in an individual living cell. These technologies include precision microwire, calcium sensor CTS-G-CaMP3 construct and modified microscopy system. This integrated single-cell analysis offers the first evidence of calcium signaling in the primary cilium of a living renal epithelium. Our data further show that cilium-dependent signaling can occur through mechanical and chemical stimulations (Fig. 6). This signaling provokes extracellular calcium influx into the cilioplasm, because fluid media without extracellular calcium fails to increase ciliary calcium (data not shown). Consistent with our previous study [3], fluid shear-induced ciliary calcium

through polycystin-2 propagates to and is amplified in the cytoplasm through the ryanodine receptor. We also provide evidence that DR5-mediated ciliary calcium signaling is mediated by the L-type calcium channel CaV1.2. Interestingly, DR5-induced ciliary calcium retains within cilioplasm, suggesting that the ciliary calcium is differentially regulated between mechanical and chemical stimuli.

Primary cilia are sensory organelles that translate extracellular stimuli into intracellular responses. Fluid-shear stress and the dopamine receptor type-5 (DR5) agonist are among the few stimuli that require cilia for intracellular calcium signal transduction. Cells without cilia are thus unable to respond to fluid-shear or DR5 agonist [2, 4, 7, 8, 20]. However, it was not known if these stimuli initiated calcium signaling within the cilium, or if the calcium signal

Fig. 5 The L-type calcium channel CaV1.2 and dopamine receptor-5 are localized to primary cilia of kidney epithelial cells. LLCPK cells were fixed, permeabilized and immunostained with L-type calcium channel (CaV1.2. **a**), dopamine receptor type-5 (DR5; **b**) or thrombin receptor (THR; **c**). Ciliary marker acetylated-α-tubulin (acet-α-tub) and nuclear DNA marker were used in all cases. To differentiate plasma membrane and ciliary localization of DR5 and THR, images were reconstructed in 3D, showing XY, XZ, and YZ planes as indicated by the *yellow arrowheads*. Whereas THR is localized in the apical membrane, DR5 and CaV1.2 are colocalized with acetylated-α-tubulin in the cilia. In all cases, merged images of *green* and *red* signals are shown with DAPI (nuclear DNA staining). *Bar* = 4 μm
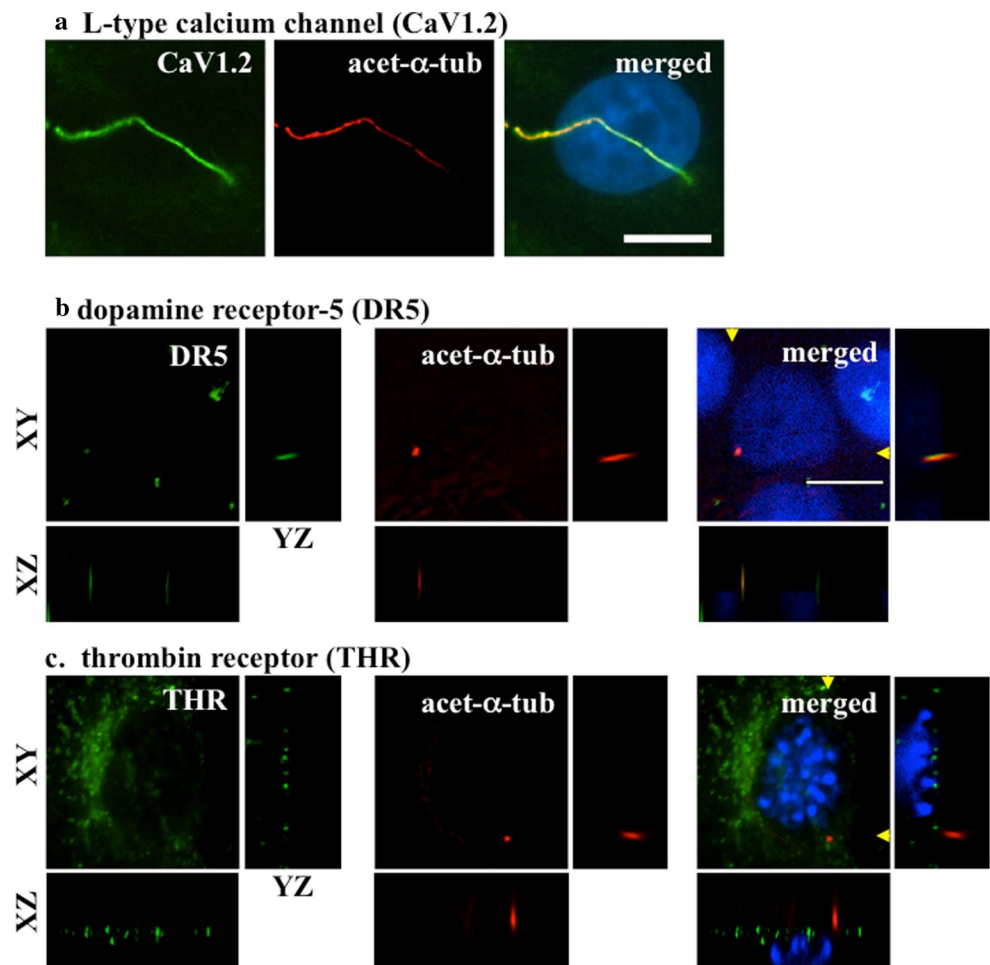

originates in the cytoplasm. We therefore selected fluid-shear and fenoldopam as cilium-dependent stimuli. We also used two cilium-independent stimuli to validate the ciliary calcium signaling. Thrombin was selected, because it distinctively and consistently showed cytosolic calcium signaling in our initial screenings. This was further supported by our previous study, in which thrombin was used as a control in our cilia-mutant renal epithelial cells [3]. Ionomycin was also selected, because it has a unique property as a non-specific calcium ionophore. While thrombin requires G protein-coupled thrombin receptor to exert its effect, ionomycin does not activate any receptor. We thus believe that these four stimuli represent a balanced approach to study ciliary signaling, although there are definitely more stimuli in which ciliary roles are worth-examined in future studies.

Our studies utilized a novel model to visualize calcium signaling within both cilioplasm and cytoplasm. More importantly, this is the very first visualization of ciliary signaling in the cilioplasm of a single-living cell. Our experimental setup was designed to permit side-view of a living cell, allowing us to examine mechanical stimulus in the cilium and cytosol simultaneously (Movies 1, 2,

and 3). We often observed two types of cytosolic calcium. The peak of cytosolic calcium could occur after the stimulus (bending) was relieved (Type I; Movie 2), or the peak of cytosolic occurred while the stimulus was occurring (Type II; Movie 3). The temporal and spatial differences between the cilioplasm and cytoplasm were therefore significant in that the peak of cytosolic calcium was delayed by 2.1 ± 0.6 s after ciliary calcium.

It is imperative to note that ryanodine receptor blockage does not inhibit sensory function of primary cilia as we previously thought [3]. Because our current single cell analysis provides a much higher temporal and spatial resolution, we are able to determine that a minute calcium spark within the cilioplasm was not affected by inhibiting ryanodine receptor indicating two possible independent yet intertwined events within the cilioplasm and cytoplasm.

We found that the baseline calcium levels in both the cilioplasm and cytoplasm are very stable, with no obvious fluorescence fluctuations in our single-cell studies. Our studies also show that the chemosensory capacity of renal epithelia can occur specifically within the cilioplasm (Movies 4 and 5) and cytoplasm (Movies 6 and 7), as confirmed
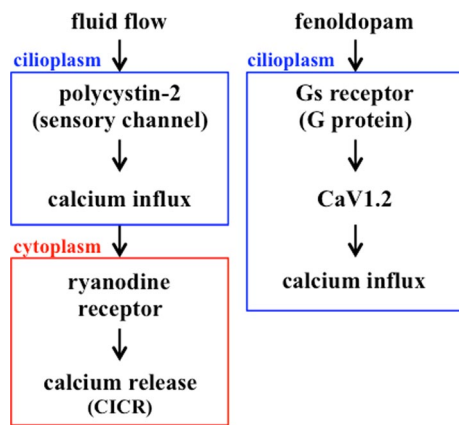
Fig. 6 Schematic of mechano- and chemosensory calcium signaling in primary cilia. Primary cilia are involved in sensing mechanical force (fluid flow) and chemical agonist (fenoldopam). Fluid flow bends a cilium and activates the polycystin-2 calcium channel, which initiates a calcium influx within the cilium. Ciliary calcium is transduced to the cytosol and amplified through the ryanodine receptor through a mechanism known as calcium-induced calcium release (CICR). Fenoldopam activates dopamine receptor-type 5, which is a Gs-coupled receptor, and promotes ciliary calcium influx through the CaV1.2 L-type calcium channel. Ciliary and cytosolic signaling is indicated in the *blue* and *red boxes*, respectively

by ionomycin control (Movies 8 and 9). It is worth mentioning that the fenoldopam-induced ciliary signal can also be observed in the proximity of the ciliary base within the cytoplasm and the thrombin-induced cytoplasmic signal can be sporadically detected at the base of a cilium. This suggests that a proportion of calcium ions are able to diffuse across the size-exclusion permeability barrier within the ciliary necklace or transition zone [21].

For the first time, we also present DR5 and CaV1.2 localizations to primary cilia of kidney epithelial cells. Although the presence of voltage-dependent channels in non-excitable cells used to be controversial, CaV1.2 mRNA has been detected and reported in renal tissue and isolated renal epithelia [22, 23]. The cilia localization further supports our functional study that CaV1.2 activation can be activated by ciliary DR5 and that blocking of CaV1.2 with verapamil can inhibit the effect of fenoldopam in primary cilia. We thus propose that the calcium signaling-induced by fenoldopam on DR5 requires CaV1.2.

In summary, the present study elucidates the dynamic process of calcium signaling in the cilium and cytosol. Although many laboratories have independently predicted that flow- or DR5-induced signaling is a cilium-mediated process [2, 4, 7, 8, 20], our present study provides the first opportunity to directly visualize calcium signaling within primary cilia. Our experimental approach will allow future studies to better understand the roles of ciliary proteins in cellular signaling and the possible downstream

pathways associated with ciliary signaling and cilia-related diseases.

Materials and methods

Plasmid construct

We used a genetically encoded indicator, G-CaMP3 to enable us to monitor intracellular calcium [24]. Of note is that none of the calcium fluorophores (e.g., Fura-2, Fluo-2, Fluo-4, and Asante Calcium Red) can be loaded into the cilioplasm due to the restriction in the ciliary transport or diffusion constraint within ciliary necklace [25]. The CTS-G-CaMP3 construct was generated using PCR to fuse the first 68 amino acids of the intracellular C-tail of fibrocystin (*Pkhd1* C1-68) to the N-terminus of the calcium indicator, G-CaMP3. G-CaMP3 was obtained from Addgene (Addgene plasmid 22692). The sequences of the fusion primers are 5′-AGT CAT GCT AGC CAT GCT CTG CAT TCC CTG-3′ and 5′-CAG GGA ATG CAG AGC ATG GCT AGC ATG ACT-3′. In addition, primers were designed to have an *Eco*RI digestion site at the 5′ end and a *Bam*HI digestion site at the 3′ end of the insert. The insert was subcloned into pcDNA3.1 (−) using these restriction sites.

Cell transfection

Cells were then transfected with the CTS-G-CaMP3 construct (0.5 μg/ml) using Xtreme6 transfection system (Roche, Inc.). In some cases, cells were co-transfected with scramble siRNA (5′- UUC UCC GAA CGU GUC ACG U-3′) or *Pkd2* siRNA (5′-GCU CCA GUG UGU ACU ACU ACA-3′) using *DharmaFECT Duo Transfection* reagent (Thermo Scientific, Inc.). All siRNAs were conjugated with Cy5 to monitor transfection efficiency. The siRNA (20 or 30 nM) provided transfection efficiency of about 80 %.

Immunostaining

LLCPK cells were immunostained using standard techniques. Briefly, cells were rinsed with 1× phosphate-buffered saline (PBS), fixed with 4 % paraformaldehyde containing 2 % sucrose for 10 min and permeabilized with 1 % Triton-X in PBS for 5 min. Acetylated-α-tubulin (1:10,000; Sigma, Inc.), CaV1.2 (1:100; Alomone Lab, Inc.), dopamine receptor-type 5 (1:2,500; Calbiochem, Inc.) or thrombin receptor (1:500; Santa Cruz, Inc.) antibody was used followed by fluorescence secondary antibody (1:500; Pierce, Inc.). Cells were counterstained with 4.6-diamidino-2-phenylindol DAPI (Vector Laboratories, Inc.). Three-dimensional images were taken with Nikon

TE2000 and reconstructed using Metamorph software, as previously described [11].

Precision microwire

A special order for the precision microwire can be obtained from H.P. Reid, Inc. in Palm Coast, FL. This wire was first coated with type I collagen, UV sterilized and mounted on a microscope coverslip (no. 1). Cells would preferentially grow on the collagen, i.e., on the wire. As needed, such wire could be gently rotated to observe the confluency of the cells around the wire. Due to its steadiness and non-toxic nature, the wire is an excellent set-up for any experimental manipulations. In our case, this includes application of fluid-shear stress and treatment of various pharmacological agents to the wire.

Live-cell imaging analysis

LLCPK cells were grown at 39 °C in Dulbecco's modified Eagle's medium containing 10 % fetal bovine serum on the precision microwire. After cells were transfected with the CTS-G-CaMP3 for 2 days, serum was withdrawn from the cell culture medium to promote ciliation. The wire-containing cells were then moved to a custom-designed perfusion chamber made of a standard 6-cm culture plate. This culture plate would basically support the inlet and outlet of fluid perfusion. More importantly, the plate would allow a tight seal of the microscope coverslip, in which the precision microwire was mounted on. Once settled on the microscope stage, the wire containing cells was equilibrated for 15–30 min.

In addition to the differential side-view imaging platform, we utilized customized high-resolution differential interference contrast (DIC) microscopy to distinctively visualize the cilium (cilioplasm) and the cell body (cytoplasm). The DIC and fluorescence images were captured using Nikon Ti-U microscope. The No. 1 microscope coverslip was used, because it is best suited for our customized 1.4 numerical aperture oil condenser lens and $60\times$ objective lens with near-infrared resolution prism. These modifications provide sharp-contrast images suitable for live-cell imaging studies on small organelles, such as cilia. For greater sensitivity, we used Photometrics Coolsnap ES2, 12-bit, 20-MHz Digital Monochrome Camera with IEEE-1394 interface. For better focusing, the microscope was equipped with XY-axis motorized flat-top inverted stage (Prior Nanopositioning Piezo Z), automatic focusing RFA Z-axis drive (digital autofocus PIFOC), and custom-designed vibration isolation platform (isolator table). For a better-controlled environment, the body of the microscope was enclosed inside a custom built chamber to control CO_2, humidity, heat and light. External stimuli were applied as described previously [26]. DIC images will be automatically adjusted for optimal brightness/contrast, exposure, and focus. Live images of CTS-G-CaMP3 were streamed at the excitation and emission wavelengths of 495 and 515 nm, respectively.

Protein analysis

LLCPK cells were homogenized in immunoprecipitation buffer (Boston Bioproducts, Inc.) according to the manufacturer's instructions. Equal amounts of protein extracts (50 μg/lane) were mixed with sample buffer and then separated on 7 % SDS-PAGE gels. Antibodies used for Western blotting included rabbit polyclonal anti-polycystin 2 (1:300; Santa Cruz Biotech, Inc.), monoclonal rabbit anti-mouse GAPDH antibody (1:10,000; Cell Signaling, Inc.) and HRP-conjugated goat anti-rabbit antibody (1:10,000; Thermo Scientific, Inc.). GAPDH was used as a loading control.

Pharmacological agents

All drugs were freshly prepared in Hank's balanced salt solution. For each drug, their optimal concentrations have been previous determined from the dose–response curve [3, 11]. Fenoldopam (DR5-specific agonist; Hospira, Inc.) or ionomycin (non-specific ionophore; Sigma Aldrich, Inc.) was applied to the cell at final concentration of 1 μM. Hexapeptide thrombin receptor agonist (Biopharm Laboratories, Inc.) was used at concentration of 1 μM with specific activity of about 1 unit/ml. Caffeine (60 μM; Fisher Scientific, Inc.) and 2-APB (10 μM; Tocris, Inc.) were used to inhibit intraorganellar ryanodine and IP_3 receptors, respectively. Verapamil (1 μM; Sigma Aldrich, Inc.) was used to inhibit CaV1.2 calcium channel. These inhibitors were incubated with the cells for an hour.

Data analysis

Experiments were repeated on at least three different sets of cell populations. For each population, three individual cells were randomly selected for analysis. For immunostaining analysis, a minimum of six coverslips (cell populations) was used for each experiment. All images were analyzed using Metamorph software. For calcium analysis, fluorescence signal intensity was first subtracted from the background fluorescence. For quantification, ciliary and cytosolic fluorescence intensities were differentially measured at each time point. To obtain proper and unbiased measurements, signal intensity was normalized to baseline fluorescence. Next, the signal intensity measured in pixel was further normalized with the total area of the measurement. To verify homogeneity of variance within each data

set (homoscedasticity), heterogeneous variances were analyzed. If detected, the data distributions were normalized via log transformation to produce normally distributed data sets for all analyses. All quantifiable data were reported as mean $\pm$ SEM. Comparisons between means were performed using ANOVA with post hoc comparisons via Dunnet, and statistical significance implies $p < 0.05$. All data analysis was done using GraphPad Prism v.5.

References

1. AbouAlaiwi WA, Takahashi M, Mell BR, Jones TJ, Ratnam S, Kolb RJ, Nauli SM (2009) Ciliary polycystin-2 is a mechanosensitive calcium channel involved in nitric oxide signaling cascades. Circ Res 104:860–869

2. Liu W, Murcia NS, Duan Y, Weinbaum S, Yoder BK, Schwiebert E, Satlin LM (2005) Mechanoregulation of intracellular Ca^{2+} concentration is attenuated in collecting duct of monocilium-impaired orpk mice. Am J Physiol Renal Physiol 289:F978–F988

3. Nauli SM, Alenghat FJ, Luo Y, Williams E, Vassilev P, Li X, Elia AE, Lu W, Brown EM, Quinn SJ et al (2003) Polycystins 1 and 2 mediate mechanosensation in the primary cilium of kidney cells. Nat Genet 33:129–137

4. Nauli SM, Kawanabe Y, Kaminski JJ, Pearce WJ, Ingber DE, Zhou J (2008) Endothelial cilia are fluid shear sensors that regulate calcium signaling and nitric oxide production through polycystin-1. Circulation 117:1161–1171

5. Nauli SM, Rossetti S, Kolb RJ, Alenghat FJ, Consugar MB, Harris PC, Ingber DE, Loghman-Adham M, Zhou J (2006) Loss of polycystin-1 in human cyst-lining epithelia leads to ciliary dysfunction. JASN 17:1015–1025

6. Praetorius HA, Spring KR (2001) Bending the mdck cell primary cilium increases intracellular calcium. J Membr Biol 184:71–79

7. Praetorius HA, Spring KR (2003) Removal of the MDCK cell primary cilium abolishes flow sensing. J Membr Biol 191:69–76

8. Siroky BJ, Ferguson WB, Fuson AL, Xie Y, Fintha A, Komlosi P, Yoder BK, Schwiebert EM, Guay-Woodford LM, Bell PD (2006) Loss of primary cilia results in deregulated and unabated apical calcium entry in ARPKD collecting duct cells. Am J Physiol Renal Physiol 290:F1320–F1328

9. Xu C, Shmukler BE, Nishimura K, Kaczmarek E, Rossetti S, Harris PC, Wandinger-Ness A, Bacallao RL, Alper SL (2009) Attenuated, flow-induced ATP release contributes to absence of flow-sensitive, purinergic Ca^{2+} signaling in human ADPKD cyst epithelial cells. Am J Physiol Renal Physiol 296:F1464–F1476

10. Abdul-Majeed S, Moloney BC, Nauli SM (2012) Mechanisms regulating cilia growth and cilia function in endothelial cells. CMLS 69:165–173

11. Abdul-Majeed S, Nauli SM (2011) Dopamine receptor type 5 in the primary cilia has dual chemo- and mechano-sensory roles. Hypertension 58:325–331

12. Praetorius HA, Praetorius J, Nielsen S, Frokiaer J, Spring KR (2004) Beta 1-integrins in the primary cilium of MDCK cells potentiate fibronectin-induced Ca^{2+} signaling. Am J Physiol Renal Physiol 287:F969–F978

13. Rondanino C, Poland PA, Kinlough CL, Li H, Rbaibi Y, Myerburg MM, Al-bataineh MM, Kashlan OB, Pastor-Soler NM, Hallows KR et al (2011) Galectin-7 modulates the length of the primary cilia and wound repair in polarized kidney epithelial cells. Am J Physiol Renal Physiol 301:F622–F633

14. Schwartz EA, Leonard ML, Bizios R, Bowser SS (1997) Analysis and modeling of the primary cilium bending response to fluid shear. Am J Physiol 272:F132–F138

15. Sharma N, Berbari NF, Yoder BK (2008) Ciliary dysfunction in developmental abnormalities and diseases. Curr Top Dev Biol 85:371–427

16. Follit JA, Li L, Vucica Y, Pazour GJ (2010) The cytoplasmic tail of fibrocystin contains a ciliary targeting sequence. J Cell Biol 188:21–28

17. Zhang MZ, Mai W, Li C, Cho SY, Hao C, Moeckel G, Zhao R, Kim I, Wang J, Xiong H et al (2004) PKHD1 protein encoded by the gene for autosomal recessive polycystic kidney disease associates with basal bodies and primary cilia in renal epithelial cells. Proc Natl Acad Sci USA 101:2311–2316

18. Marley A, von Zastrow M (2010) Disc1 regulates primary cilia that display specific dopamine receptors. PLoS ONE 5:e10902

19. Muntean BS, Horvat CM, Behler JH, Aboualaiwi WA, Nauli AM, Williams FE, Nauli SM (2010) A comparative study of embedded and anesthetized zebrafish in vivo on myocardial calcium oscillation and heart muscle contraction. Frontiers Pharmacol 1:139

20. Masyuk AI, Masyuk TV, Splinter PL, Huang BQ, Stroope AJ, LaRusso NF (2006) Cholangiocyte cilia detect changes in luminal fluid flow and transmit them into intracellular Ca^{2+} and camp signaling. Gastroenterology 131:911–920

21. Kee HL, Dishinger JF, Blasius TL, Liu CJ, Margolis B, Verhey KJ (2012) A size-exclusion permeability barrier and nucleoporins characterize a ciliary pore complex that regulates transport into cilia. Nat Cell Biol 14:431–437

22. Nakagawa T, Yamaguchi M (2006) Overexpression of regucalcin enhances its nuclear localization and suppresses l-type Ca^{2+} channel and calcium-sensing receptor MRNA expressions in cloned normal rat kidney proximal tubular epithelial NRK52E cells. J Cell Biochem 99:1064–1077

23. Zhao PL, Wang XT, Zhang XM, Cebotaru V, Cebotaru L, Guo G, Morales M, Guggino SE (2002) Tubular and cellular localization of the cardiac l-type calcium channel in rat kidney. Kidney Int 61:1393–1406

24. Tian L, Hires SA, Mao T, Huber D, Chiappe ME, Chalasani SH, Petreanu L, Akerboom J, McKinney SA, Schreiter ER et al (2009) Imaging neural activity in worms, flies and mice with improved GCaMP calcium indicators. Nat Methods 6:875–881

25. Vieira OV, Gaus K, Verkade P, Fullekrug J, Vaz WL, Simons K (2006) FAPP2, cilium formation, and compartmentalization of the apical membrane in polarized Madin–Darby canine kidney (MDCK) cells. Proc Natl Acad Sci USA 103:18556–18561

26. Nauli SM, Jin X, AbouAlaiwi WA, El-Jouni W, Su X, Zhou J (2013) Non-motile primary cilia as fluid shear stress mechanosensors. Methods Enzymol 525:1–20